molecules

MDPI

Article

Solubility Data of the Bioactive Compound Piperine in (Transcutol + Water) Mixtures: Computational Modeling, Hansen Solubility Parameters and Mixing Thermodynamic Parameters

Faiyaz Shakeel, Nazrul Haq and Sultan Alshehri *

Department of Pharmaceutics, College of Pharmacy, King Saud University, P.O. Box 2457, Riyadh 11451, Saudi Arabia; faiyazs@fastmail.fm (F.S.); nazrulhaq59@gmail.com (N.H.)
* Correspondence: salshehri1@ksu.edu.sa

Academic Editor: William E. Acree, Jr.
Received: 28 May 2020; Accepted: 11 June 2020; Published: 13 June 2020

Abstract: The solubility values and thermodynamic parameters of a natural phytomedicine/nutrient piperine (PPN) in Transcutol-HP (THP) + water combinations were determined. The mole fraction solubilities (x_e) of PPN in THP + water combinations were recorded at T = 298.2–318.2 K and p = 0.1 MPa by the shake flask method. Hansen solubility parameters (HSPs) of PPN, pure THP, pure water and THP + water mixtures free of PPN were also computed. The x_e values of PPN were correlated well with "Apelblat, Van't Hoff, Yalkowsky–Roseman, Jouyban–Acree and Jouyban–Acree–Van't Hoff" models with root mean square deviations of < 2.0%. The maximum and minimum x_e value of PPN was found in pure THP (9.10×10^{-2} at T = 318.2 K) and pure water (1.03×10^{-5} at T = 298.2 K), respectively. In addition, HSP of PPN was observed more closed with that of pure THP. The thermodynamic parameters of PPN were obtained using the activity coefficient model. The results showed an endothermic dissolution of PPN at m = 0.6–1.0 in comparison to other THP + water combinations studied. In addition, PPN dissolution was recorded as entropy-driven at m = 0.8–1.0 compared with other THP + water mixtures evaluated.

Keywords: activity coefficient model; bioactive compound; piperine; solubility; solution thermodynamics; Transcutol

1. Introduction

Piperine (PPN; Figure 1) is a bioactive alkaloidal phytomedicine/nutrient that is present in the fruits and roots of *Piper nigrum* and *Piper longum* [1,2]. The pungency and bitter taste of pepper are due to the presence of PPN [2]. PPN is a potent bioactive compound, which has been reported to have several therapeutic activities including "anti-metastatic [3], enzyme activity stimulator [4], antimicrobial [5], antifertility [6], hepatoprotective [7], antiulcer [8], antiamoebic [9], antidiarrheal [10], anti-fibrotic [11], antifungal [12], acaricidal [13], anti-inflammatory [14,15], antioxidant [2,16,17] and anticancer activity [2,18]". In addition, PPN has also been reported as a permeation and bioavailability enhancer for several weakly soluble drugs as well as nutrients [1,2,19–21]. The solubilization of phytomedicines/nutrients in co-solvent–water mixtures had significant role in their "isolation, extraction, purification, recrystallization, drug discovery and dosage form design" [22–24]. Therefore, the solubilization of PPN in co-solvent–water mixtures should be studied in order to obtain its application in pharmaceutical and food industries. Transcutol-HP (THP) is a potential co-solvent that is miscible with all proportions of water [24,25]. Its potential in increasing the solubilization of several poorly soluble bioactive compounds including vanillin, reserpine, sinapic acid and apigenin has been very well reported in the literature [24–27]. Some formulation technologies including solid

dosage forms [28,29], emulsion/self-emulsifying formulations [30–32], nanomedicine-based drug delivery systems [33–36] and solid dispersion technology [37] have been studied in order to enhance solubility and bioactivity/bioavailability of PPN. The solubility of PPN in pure solvents including pure water, pure propylene glycol (PG), pure polyethylene glycol-400 (PEG-400) and pure THP at ambient temperature was reported elsewhere [1,30,31]. The solubility and mixing thermodynamic parameters of PPN in twelve different pure solvents including "water, methanol, ethanol, isopropanol, 1-butanol, 2-butanol, ethylene glycol, PG, PEG-400, ethyl acetate, dimethyl sulfoxide and THP" at "T = 298.2–318.2 K" and "p = 0.1 MPa" have also been reported [38]. The solubility data of PPN in water–ethanol and water–surfactant mixtures was also found elsewhere [39–41]. The solubility values of PPN in super critical carbon dioxide (CO_2) and near critical CO_2 at different temperatures has also been reported elsewhere [42]. So far, there is no report on PPN solubilization in "THP + water" mixtures at "T = 298.2–318.2 K" and "p = 0.1 MPa". Therefore, in this research, the solubility profile of PPN in various "THP + water" mixtures, including pure water and pure THP at "T = 298.2–318.2 K" and "p = 0.1 MPa" is studied and reported. Mixing thermodynamic parameters of PPN are also computed and reported using an activity coefficient model. The solubility values of PPN reported in this research could be beneficial in "isolation, extraction, purification, recrystallization, drug discovery, pre-formulation studies and dosage form design" of PPN.

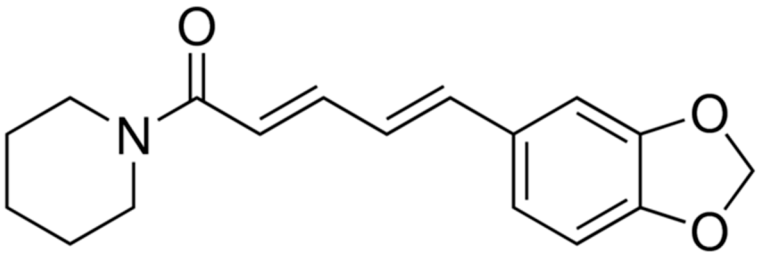

Figure 1. Chemical structure of piperine (PPN).

2. Results and Discussion

2.1. Experimental Solubility Values of PPN and Literature Comparison

The "mole fraction solubility (x_e)" values of PPN in various "THP + water" combinations including pure water and pure THP at "T = 298.2–318.2 K' and "p = 0.1 MPa" are summarized in Table 1. The solubility values of PPN in pure water and pure THP have been reported [38]. However, its solubility values in "THP + water" mixtures have not been reported elsewhere so far.

The solubility of PPN in pure water at "T = 298.2 K" was recorded as 0.164 mg g^{-1} (equivalent to $x_e = 1.04 \times 10^{-5}$) and 10 µg g^{-1} (equivalent to $x_e = 6.31 \times 10^{-7}$) by Shao et al. and Veerareddy et al., respectively [30,31]. In addition, the solubility of PPN in water at "T = 291.2 K" was obtained as 40 µg g^{-1} (equivalent to $x_e = 2.53 \times 10^{-6}$) by another report [1]. The x_e value of PPN in pure water at "T = 298.2 K" was calculated as 1.03×10^{-5} in the current research (Table 1). The solubility of PPN in pure THP at "T = 298.2 K" was obtained as 185.29 mg g^{-1} (equivalent to $x_e = 8.01 \times 10^{-2}$) [31]. The x_e value of PPN in pure THP at "T = 298.2 K" was calculated as 7.88×10^{-2} in the current research (Table 1). The x_e values of PPN in pure water and pure THP obtained in the current research were found to be very close to those reported by Shao et al. [31]. However, the x_e value of PPN in pure water obtained in the current research was found to have deviated much from those reported by Veerareddy et al. and Vasavirama and Upender [1,30]. This deviation could be due to the variation in shaking speed, equilibrium time and analysis method of PPN [1,30,38]. The solubility values of PPN in pure water and pure THP at five different temperatures, i.e., "T = 298.2–318.2 K" have also been reported [38]. The graphical comparison between x_e and literature solubility values of PPN in pure water and pure THP at "T = 298.2–318.2 K" are summarized in Figure 2A,B, respectively. The data summarized in Figure 2A,B suggested an excellent correlation of x_e values of PPN with the literature solubility data

of PPN in pure water and pure THP at "T = 298.2–318.2 K". Overall, the experimental solubility values of PPN obtained in the current research were found in good agreement with those reported in the literature. The reliability of the proposed method of solubility measurement was verified by obtaining the x_e values of another phytomedicine/nutraceutical apigenin in pure THP at T = 298.2 K and T = 318.2 K. The x_e value of apigenin in pure THP at T = 298.2 K and T = 318.2 K was found as 3.36×10^{-1} and 3.82×10^{-1}, respectively, in the literature [27]. The x_e value of apigenin in pure THP at T = 298.2 K and T = 318.2 K was determined as 3.33×10^{-1} and 3.84×10^{-1}, respectively, in the current research. These results suggested that the x_e value of apigenin in pure THP obtained using the current technique was very close to those reported in the literature [27]. Therefore, the present technique of solubility measurement was reliable for the solubility determination of PPN.

Table 1. Experimental solubilities (x_e) of piperine (PPN) in mole fraction in different "Transcutol-HP (THP) + water" mixtures (m) at "T = 298.2–318.2 K" and "p = 0.1 MPa" [a].

m	x_e				
	T = 298.2 K	T = 303.2 K	T = 308.2 K	T = 313.2 K	T = 318.2 K
0.0	1.03×10^{-5}	1.17×10^{-5}	1.31×10^{-5}	1.47×10^{-5}	1.59×10^{-5}
0.1	2.57×10^{-5}	2.85×10^{-5}	3.19×10^{-5}	3.55×10^{-5}	3.80×10^{-5}
0.2	6.20×10^{-5}	6.88×10^{-5}	7.61×10^{-5}	8.40×10^{-5}	9.01×10^{-5}
0.3	1.59×10^{-4}	1.71×10^{-4}	1.86×10^{-4}	1.99×10^{-4}	2.15×10^{-4}
0.4	3.71×10^{-4}	4.07×10^{-4}	4.42×10^{-4}	4.79×10^{-4}	5.09×10^{-4}
0.5	9.06×10^{-4}	9.80×10^{-4}	1.08×10^{-3}	1.16×10^{-3}	1.25×10^{-3}
0.6	2.23×10^{-3}	2.39×10^{-3}	2.56×10^{-3}	2.74×10^{-3}	2.88×10^{-3}
0.7	5.40×10^{-3}	5.74×10^{-3}	6.10×10^{-3}	6.51×10^{-3}	6.80×10^{-3}
0.8	1.35×10^{-2}	1.40×10^{-2}	1.47×10^{-2}	1.55×10^{-2}	1.63×10^{-2}
0.9	3.26×10^{-2}	3.37×10^{-2}	3.53×10^{-2}	3.70×10^{-2}	3.87×10^{-2}
1.0	7.88×10^{-2}	8.12×10^{-2}	8.44×10^{-2}	8.79×10^{-2}	9.10×10^{-2}
x^{idl}	5.13×10^{-2}	6.02×10^{-2}	7.06×10^{-2}	8.26×10^{-2}	9.63×10^{-2}

[a] The relative uncertainties u_r are $u_r(T) = 0.010$, $u_r(m) = 0.001\%$, $u(p) = 0.003$ and $u_r(x_e) = 0.11$.

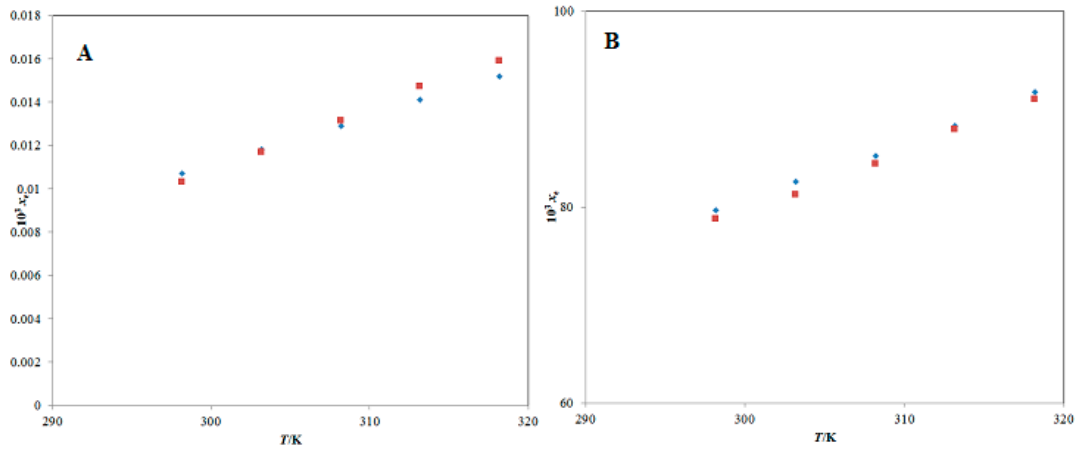

Figure 2. Comparison of mole fraction solubility of PPN in (**A**) pure water and (**B**) pure Transcutol-HP (THP) with reported solubilities at "T = 298.2 K to 318.2 K"; the symbol ■ shows the experimental mole fraction solubility of PPN in (**A**) pure water and (**B**) pure THP, and the symbol ◆ shows the reported solubilities of PPN in (**A**) pure water and (**B**) pure THP taken from reference [38].

As per the results summarized in Table 1, the x_e values of PPN were found to increase with increases in both THP mass fraction (m) in various "THP + water" combinations and temperature, and therefore the minimum x_e value of PPN was obtained in pure water ($x_e = 1.03 \times 10^{-5}$) at "$T$ = 298.2 K", and the maximum x_e value of PPN was observed in pure THP ($x_e = 9.10 \times 10^{-2}$) at "$T$ = 318.2 K". The maximum x_e value of PPN in pure THP could be due to the lower polarity and low Hansen solubility parameter

(HSP) of THP in comparison to high polarity and higher HSP of water [25,26]. The impact of *m* value of THP on PPN solubility at "*T* = 298.15–318.15 K" is summarized in Figure 3.

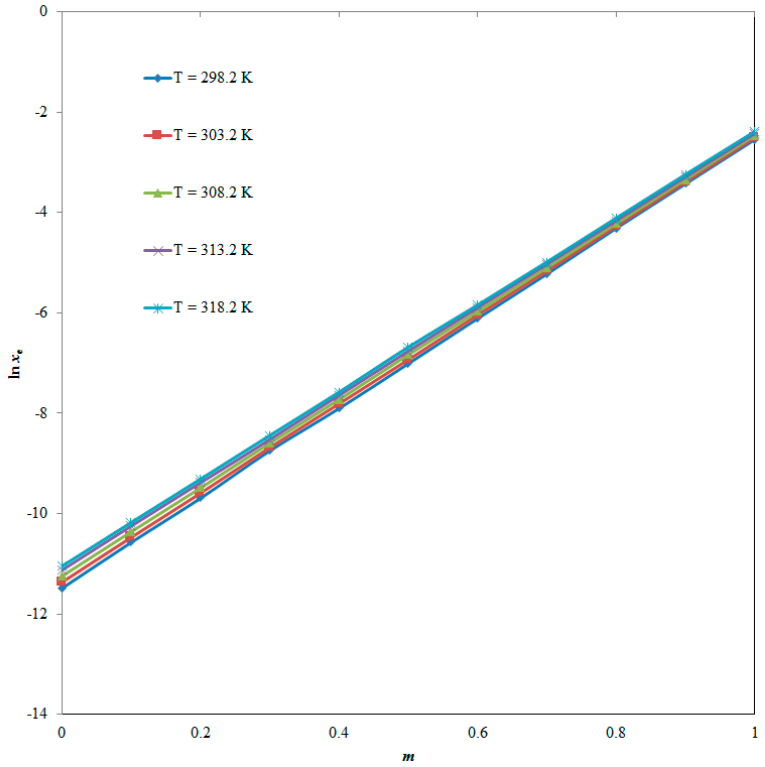

Figure 3. Effect of mass fraction of THP (*m*) on solubility of PPN at "*T* = 298.2–318.2 K".

As per these results, the PPN solubility was found to increase linearly with increases in *m* values of THP at all five temperatures studied. It was also observed that the x_e values of PPN were significantly enhanced from pure water to pure THP, and therefore THP could be utilized as an excellent co-solvent in PPN solubility enhancement.

2.2. Hansen Solubility Parameters (HSPs)

The results of HSPs of different "THP + water" systems free of PPN are tabulated in Supplementary Materials Table S1. The HSP (δ) value of PPN was computed as 22.30 $MPa^{1/2}$. The HSP value for pure THP (δ_1) and pure water (δ_2) were computed as 21.40 and 47.80 $MPa^{1/2}$, respectively. The HSP values for various "THP + water" mixtures free of PPN (δ_{mix}) were computed as 24.04–45.16 $MPa^{1/2}$. As per the data recorded, the HSP value of pure THP (δ_2 = 21.40 $MPa^{1/2}$) and "THP + water" mixtures (at *m* = 0.9; δ_{mix} = 24.04 $MPa^{1/2}$) were found to close to that of PPN (δ = 22.30 $MPa^{1/2}$). The x_e values of PPN were also obtained at the maximum in pure THP and at *m* = 0.9 of THP in "THP + water" mixtures. Hence, the obtained solubility data of PPN in various "THP + water" mixtures was in good agreement with their HSPs

2.3. Mixing Thermodynamic Parameters of PPN Solution

The computed values of various mixing thermodynamic parameters such as "mixing Gibbs energy ($\Delta_{mix}G$), mixing enthalpy ($\Delta_{mix}H$) and mixing entropy ($\Delta_{mix}S$)" along with activity coefficients (γ_i) for PPN in different "THP + water" combinations including pure water and pure THP are given in Supplementary Materials Table S2. The $\Delta_{mix}G$ values for PPN at *m* = 0.6–1.0 were found as negative values, which decreased with the increase in temperature. Hence, PPN dissolution was proposed as endothermic at *m* = 0.6–1.0. The $\Delta_{mix}S$ values for PPN at *m* = 0.8–1.0 were found as positive values,

which also decreased with increases in temperature. Therefore, PPN dissolution was proposed as entropy-driven at m = 0.8–1.0. The $\Delta_{mix}H$ values for PPN were found as negative values in most of the "THP + water" combinations studied.

2.4. Solute–Solvent Molecular Interactions

The data of γ_i for PPN in different "THP + water" combinations including pure water and pure THP at "T = 298.2–318.2 K" is summarized in Table 2. The γ_i value obtained for PPN was highest in pure water at all five temperatures studied. However, the γ_i value obtained for PPN was lowest in pure THP at all five temperatures. The highest γ_i value for PPN in pure water could be possible due to the lowest x_e value of PPN in pure water. As per these results, the γ_i value for PPN was found to increase with increases in temperature in all "THP + water" mixtures studied. Based on these results, the maximum solute–solvent interactions were considered in PPN–THP compared with PPN–water.

Table 2. Activity coefficients (γ_i) of PPN in different "THP + water" mixtures (m) at "T = 298.2–318.2 K".

m	γ_i				
	T = 298.2 K	T = 303.2 K	T = 308.2 K	T = 313.2 K	T = 318.2 K
0.0	4980.00	5150.00	5380.00	5620.00	6050.00
0.1	1995.20	2108.92	2215.74	2339.59	2533.27
0.2	827.00	875.00	927.00	984.00	1070.00
0.3	322.00	353.00	380.00	416.00	448.00
0.4	138.00	148.00	160.00	173.00	189.00
0.5	56.60	61.40	65.50	71.40	77.30
0.6	23.00	25.20	27.60	30.20	33.40
0.7	5.40	5.74	6.10	6.51	6.80
0.8	3.81	4.31	4.82	5.33	5.92
0.9	1.57	1.79	2.00	2.23	2.49
1.0	0.65	0.74	0.83	0.94	1.06

2.5. Modeling of PPN Solubility

The solubility data obtained for PPN was correlated using "Van't Hoff, Apelblat, Yalkowsky–Roseman, Jouyban–Acree and Jouyban–Acree–Van't Hoff" models [26,43–48]. Results of the "Van't Hoff model" for PPN in different "THP + water" mixtures including pure water and pure THP are summarized in Table 3.

Table 3. Results of "Van't Hoff model" for PPN in "THP + water" combinations (m) [b].

m	a	b	R^2	*RMSD* (%)	Overall *RMSD* (%)
0.0	−4.45	−2093.60	0.9960	1.11	
0.1	−4.20	−1897.30	0.9963	0.91	
0.2	−3.65	−1799.00	0.9973	0.70	
0.3	−3.98	−1421.50	0.9982	0.33	
0.4	−2.83	−1509.30	0.9968	0.62	
0.5	−1.90	−1520.50	0.9981	0.77	0.65
0.6	−1.95	−1238.70	0.9985	0.42	
0.7	−1.49	−1112.00	0.9973	0.42	
0.8	−1.24	−916.75	0.9935	0.56	
0.9	−0.64	−829.34	0.9932	1.01	
1.0	−0.21	−696.21	0.9960	0.31	

[b] The average relative uncertainties are $u(a)$ = 0.30 and $u(b)$ = 0.07.

The graphical correlation between x_e and "Van't Hoff model solubility ($x^{Van't}$)" of PPN is presented in Supplementary Materials Figure S1, which shows good graphical correlation. The root mean square deviations (*RMSDs*) for PPN in various "THP + water" combinations including pure water and pure

THP were recorded as 0.31–1.11% with an average *RMSD* of 0.65%. In addition, the determination coefficients (R^2) were obtained as 0.9935–0.9985.

The results of the "Apelblat model" for PPN in different "THP + water" mixtures including pure water and pure THP are summarized in Table 4.

Table 4. Results of "Apelblat model" for PPN in "THP + water" combinations (m) [c].

m	*A*	*B*	*C*	R^2	*RMSD* (%)	Overall *RMSD* (%)
0.0	331.19	−17,505.00	−49.84	0.9995	0.78	
0.1	224.66	−12,407.50	−33.98	0.9982	0.73	
0.2	217.93	−11,974.50	−32.90	0.9993	0.58	
0.3	−105.09	3214.87	15.01	0.9988	0.57	
0.4	228.14	−12,114.70	−34.29	0.9999	0.60	
0.5	45.42	−3697.43	−7.02	0.9981	0.45	0.54
0.6	87.58	−5351.77	−13.29	0.9991	0.34	
0.7	84.34	−5054.78	−12.74	0.9981	0.44	
0.8	−157.86	6268.79	23.26	0.9978	0.61	
0.9	−157.97	6388.73	23.36	0.9985	0.45	
1.0	−84.70	3179.61	12.54	0.9982	0.47	

[c] The average relative uncertainties are $u(A) = 0.92$, $u(B) = 1.54$ and $u(C) = 0.90$.

The graphical correlation between x_e and "Alelblat model solubility (x^{Apl})" values of PPN are presented in Figure 4, which expressed good graphical correlation.

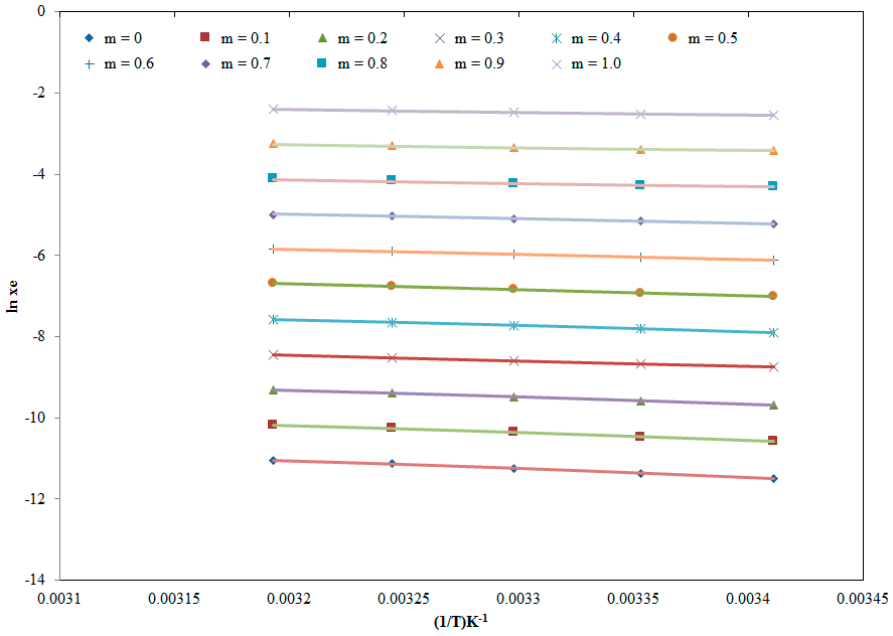

Figure 4. Correlation of experimental solubility values of PPN with "Apelblat model" in different "THP + water" mixtures at "T = 298.2–318.2 K"; Apelblat model solubility values of PPN are represented by solid lines, and experimental solubility values of PPN are represented by the symbols.

The *RMSD*s for PPN in various "THP + water" combinations including pure water and pure THP were estimated as 0.34–0.78% with an average *RMSD* of 0.54%. In addition, the R^2 values were estimated as 0.9978–0.9999.

Results of the "Yalkowsky–Roseman model" for PPN in different "THP + water" combinations are listed in Table 5. The *RMSD* values for PPN in different "THP + water" combinations were computed as 0.46–2.81% with an average *RMSD* of 1.24%.

Table 5. Results of "Yalkowsky–Roseman model" for PPN in different "THP + water" mixtures (*m*) at "*T* = 298.2–318.2 K".

m	Log x^{Yal}					*RMSD* (%)	Overall *RMSD* (%)
	T = 298.2 K	*T* = 303.2 K	*T* = 308.2 K	*T* = 313.2 K	*T* = 318.2 K		
0.1	−4.59	−4.54	−4.50	−4.45	−4.42	1.21	
0.2	−4.21	−4.16	−4.12	−4.07	−4.04	0.46	
0.3	−3.82	−3.77	−3.74	−3.69	−3.67	2.81	
0.4	−3.43	−3.39	−3.35	−3.32	−2.29	0.91	
0.5	−3.04	−3.01	−2.97	−2.94	−2.91	2.27	1.24
0.6	−2.65	−2.62	−2.59	−2.56	−2.54	1.11	
0.7	−2.26	−2.24	−2.21	−2.18	−2.16	0.38	
0.8	−1.88	−1.85	−1.83	−1.81	−1.79	1.31	
0.9	−1.49	−1.47	−1.45	−1.43	−1.41	0.78	

Results of the "Jouyban–Acree model" for PPN in "THP + water" mixtures are listed in Table 6. The average *RMSD* for PPN was estimated as 0.42%.

Table 6. Results of "Jouyban–Acree" and "Jouyban–Acree–Van't Hoff" models for PPN in "THP + water" combinations.

System	Jouyban–Acree	Jouyban–Acree–Van't Hoff
PEG-400 + water	J_i–14.43	A_1–0.21 B_1–696.21 A_2–4.45 B_2–2093.60 J_i–16.42
RMSD (%)	0.42	
		0.54

Results of the "Jouyban–Acree–Van't Hoff model" for PPN in "THP + water" mixtures are tabulated in Table 6. The average *RMSD* for PPN was estimated as 0.54%.

As per the results recorded for solubility modeling, it was observed that all investigated models showed low *RMSD*s (average *RMSD* < 2.0%), which indicated good correlation of obtained solubility data of PPN with all investigated models. However, it should be noted that the error values of every model could not be compared with each other as each model was related with different parameters and model coefficients [49]. In general, the performance of all investigated models was good, but the "Jouyban–Acree model" could be considered as the most suitable model because it utilized the least number of model coefficients in addition to having a low *RMSD* value.

3. Experimental

3.1. Materials

PPN and THP were procured from "Beijing Mesochem Technology Co. Pvt. Ltd. (Beijing, China)" and "Gattefosse (Lyon, France)", respectively. Water was collected from a Milli-Q water purification unit. The properties of materials are listed in Table 7.

Table 7. List of materials used.

Material	Molecular Formula	Molar Mass (g mol^{-1})	CAS Registry No.	Purification Method	Mass Fraction Purity	Analysis Method	Analysis Method	Source
PPN	$C_{17}H_{19}NO_3$	285.34	94-62-2	None	>0.99	HPLC	HPLC	Sigma Aldrich
THP	$C_6H_{14}O_3$	134.17	111-90-0	None	>0.99	GC	GC	Gattefosse
Water	H_2O	18.07	7732-18-5	None	-	-	-	Milli-Q

Purity and method of analysis were provided by supplier of each material.

3.2. PPN Solubility Measurement

A well-known saturation shake flask method was applied to measure the solubility of PPN in various "THP + water" combinations (m = 0.1–0.9) including pure water (m = 0.0) and pure THP (m = 1.0) [50]. This study was performed at "T = 298.2–318.2 K" and "p = 0.1 MPa", and each study was repeated at least for three times. Excess PPN powder was taken into glass vials having 1.0 g of each "THP + water" mixtures including pure solvents. All the prepared samples were transferred to a "OLS 200 Grant Scientific Biological Shaker (Grant Scientific, Cambridge, UK)" after temperature and shaker speed settings. After equilibrium, the samples were removed from the shaker, centrifuged and diluted using methanol (mobile phase) and utilized for the determination of PPN content using the reported high-performance liquid chromatography method at 254 nm [38]. The amount of PPN in each sample was determined using a calibration curve of PPN. The x_e values of PPN were calculated using Equations (1) and (2) [26,27]:

$$x_e = \frac{m_1/M_1}{m_1/M_1 + m_2/M_2} \quad (1)$$

$$x_e = \frac{m_1/M_1}{m_1/M_1 + m_2/M_2 + m_3/M_3} \quad (2)$$

Here, m_1 = PPN mass; m_2 = THP mass; m_3 = water mass; M_1 = PPN molar mass; M_2 = THP molar mass and M_3 = water molar mass. PPN solubility in pure water and pure THP was computed by applying Equation (1). PPN solubility in "THP + water" mixtures was calculated using Equation (2).

3.3. Computation of HSPs

If the solubility parameter of the solute is close to that of pure solvents or cosolvent mixtures, the solubility of solute will be higher in that particular pure solvent or cosolvent mixtures [51]. Therefore, HSPs for PPN, pure THP, pure water and various "THP + water" mixtures free of PPN were computed in this research. The δ value for PPN, pure THP and pure water was computed by applying Equation (3) [49,51,52] as follows:

$$\delta^2 = \delta_d^2 + \delta_p^2 + \delta_h^2 \quad (3)$$

in which "δ = total HSP; δ_d = dispersion HSP; δ_p = polar HSP and δ_h = hydrogen-bonded HSP". The HSPs for PPN, pure THP and pure water were estimated using "HSPiP software (version 4.1.07, Louisville, KY, USA)" [51]. The HSPs of various "THP + water" mixtures free of PPN (δ_{mix}) were calculated using Equation (4) [26,53] as follows:

$$\delta_{mix} = \propto \delta_1 + (1 - \propto)\delta_2 \quad (4)$$

Here, α = volume fraction of THP in "THP + water" mixtures; δ_1 = HSP of pure THP and δ_2 = HSP of pure water.

3.4. Mixing Thermodynamics Parameters of PPN Solution

Different mixing thermodynamic parameters of PPN solution were computed using the "Lewis–Randall rule". For an ideal solution, different mixing thermodynamic parameters such as "mixing Gibbs energy ($\Delta_{mix}G^{id}$), mixing entropy ($\Delta_{mix}S^{id}$) and mixing enthalpy ($\Delta_{mix}H^{id}$)" in different "THP + water" mixtures including pure water and pure THP can be calculated using Equations (5)–(7) [54,55] as follows:

$$\Delta_{mix}G^{id} = RT\ (x_1 \ln x_1 + x_2 \ln x_2 + x_3 \ln x_3) \quad (5)$$

$$\Delta_{mix}S^{id} = -R\ (x_1 \ln x_1 + x_2 \ln x_2 + x_3 \ln x_3) \quad (6)$$

$$\Delta_{mix}H^{id} = 0 \quad (7)$$

Here, R = universal gas constant (R = 8.314 J/mol/K); x_1 = PPN mole fraction; x_2 = THP mole fraction and x_3 = water mole fraction.

For a non-ideal solution, various mixing thermodynamic parameters such as $\Delta_{mix}G$, $\Delta_{mix}H$ and $\Delta_{mix}S$ in different "THP + water" mixtures including pure water and pure THP can be calculated using Equations (8)–(10) [54–56] as follows:

$$\Delta_{mix}G = \Delta_{mix}G^{id} + G^{E} \quad (8)$$

$$\Delta_{mix}H = \Delta_{mix}H^{id} + H^{E} \quad (9)$$

$$\Delta_{mix}H = \Delta_{mix}H^{id} + H^{E} \quad (10)$$

Here, G^E = excess Gibbs energy and H^E = excess enthalpy. The G^E and H^E values were computed using the activity coefficient-based Wilson model by applying Equations (11) and (12) [56,57] as follows:

$$G^{E} = RT\ (x_1 \ln \gamma_i + x_2 \ln \gamma_i + x_3 \ln \gamma_i) \quad (11)$$

$$H^{E} = -T^2\left[\partial\left(\frac{G^{E}/T}{\partial T}\right)\right] \quad (12)$$

The γ_i value for PPN in different THP + water combinations including pure water and pure THP was calculated by applying Equation (13) [58–60] as follows:

$$\gamma_i = \frac{x^{idl}}{x_e} \quad (13)$$

Here, x^{idl} = ideal solubility of PPN which was computed using Equation (14) [58] as follows:

$$\ln x^{idl} = \frac{-\Delta H_{fus}(T_{fus} - T)}{RT_{fus}T} + \left(\frac{\Delta C_p}{R}\right)\left[\frac{T_{fus} - T}{T} + \ln\left(\frac{T}{T_{fus}}\right)\right] \quad (14)$$

Here, ΔC_p = difference between the molar heat capacity of solid state and liquid state; T_{fus} = fusion temperature of PPN and ΔH_{fus} = fusion enthalpy of PPN [59,61]. The values of T_{fus}, ΔH_{fus} and ΔC_p for PPN were taken as 404.88 K, 32.69 kJ mol^{-1} and 80.74 J mol^{-1} K^{-1}, respectively, from reference [38].

3.5. Solute–Solvent Molecular Interactions

The molecular interactions between PPN and various "THP + water" mixtures including pure water and pure THP can be explained using activity coefficients values. The γ_i values for PPN in different "THP + water" mixtures and pure solvents at "T = 298.2–318.2 K" were calculated by applying Equation (13) listed above.

3.6. Thermodynamics-Based Computational Models

The solubility value obtained in the current research for PPN in various "THP + water" combinations including pure solvents was correlated using "Van't Hoff, Apelblat, Yalkowsky–Roseman, Jouyban–Acree and Jouyban–Acree–Van't Hoff" models [26,43–48]. The $x^{\text{Van't}}$ value of PPN in different "THP + water" mixtures including pure water and pure THP was calculated by applying Equation (15) [26] as follows:

$$\ln x^{\text{Van't}} = a + \frac{b}{T} \tag{15}$$

in which a and b = model coefficients of Equation (15), which were determined by the graphs constructed between ln x_e of PPN and 1/T. The correlation between x_e and $x^{\text{Van't}}$ values of PPN was carried out using *RMSD* and R^2. The *RMSD*s of for PPN were calculated using its formula reported previously in the literature [27]. The x^{Apl} value of PPN in various "THP + water" combinations including pure water and pure THP was calculated using Equation (16) [43,44].

$$\ln x^{\text{Apl}} = A + \frac{B}{T} + C\ln(T) \tag{16}$$

Here, A, B and C = the model coefficients of Equation (16), which were obtained using "nonlinear multivariate regression analysis" of x_e values of PPN summarized in Table 1 [26]. The correlation between x_e and x^{Apl} values of PPN was again performed using *RMSD* and R^2. The logarithmic solubility of "Yalkowsky–Roseman model (log x^{Yal})" for PPN in various "THP + water" mixtures was calculated by applying Equation (17) [45] as follows:

$$\log x^{\text{Yal}} = m_1 log x_1 + m_2 log x_2 \tag{17}$$

Here, x_1 = mole fraction solubility of PPN in THP; x_2 = mole fraction solubility of PPN in water; m_1 = THP mass fraction and m_2 = water mass fraction.

The "Jouyban–Acree model solubility ($x_{m,T}$)" of PPN in different "THP + water" combinations was calculated by applying Equation (18) [62–64] as follows:

$$\ln\ x_{\text{m,T}} = m_1 \ln x_1 + m_2 \ln x_2 + \left[\frac{m_1\, m_2}{T}\sum_{i=0}^{2} J_{\text{i}}(m_1 - m_2)\right] \tag{18}$$

Here, J_{i} = model coefficient of Equation (18) which was obtained using "no-intercept regression analysis" [65,66]. Based on the current data set, the trained version of Equation (18) can be expressed using Equation (19).

$$\ln\ x_{\text{m,T}} = m_1 \ln x_1 + m_2\ \ln\ x_2 + \frac{-14.43 m_1\, m_2}{T} \tag{19}$$

The correlation between x_e and $x_{m,T}$ of PPN was conducted using *RMSD*. The "Jouyban–Acree–Van't Hoff model solubility of PPN ($x_{m,T}$)" in different "THP + water" combinations was calculated by applying Equation (20) [26,66] as follows:

$$\ln\ x_{\text{m,T}} = m_1\left(A_1 + \frac{B_1}{T}\right) + m_2\left(A_2 + \frac{B_2}{T}\right) + \left[\frac{m_1 m_2}{T}\ \sum_{i=0}^{2} J_{\text{i}}(m_1 - m_2)\right] \tag{20}$$

Here, A_1, B_1, A_2, B_2 and J_i = the model coefficient of Equation (20). Based on the current data set, the trained version of Equation (20) can be expressed using Equation (21).

$$\ln\ x_{\text{m,T}} = m_1\left(-0.21 - \frac{-696.21}{T}\right) + m_2\left(-4.45 - \frac{-2093.60}{T}\right) + \frac{-16.42 m_1 m_2}{T} \tag{21}$$

4. Conclusions

This study was aimed to determine the solubility of a bioactive compound PPN in various "THP + water" combinations including pure water and pure THP at "T = 298.2–318.2 K" and "p = 0.1 MPa". The solubility of PPN was recorded as increasing with arise in both m value of THP and temperature in all "THP + water" mixtures including pure water and pure THP. Obtained solubility data of PPN was correlated well by "Apelblat, Van't Hoff, Yalkowsky–Roseman, Jouyban–Acree and Jouyban–Acree–Van't Hoff" models with an average *RMSD* of <2.0%. Overall, the "Jouyban–Acree model" was found as the most suitable for this modeling. The maximum solute–solvent interactions were observed in the PPN–THP combination in comparison to PPN–water. The results of mixing thermodynamics showed an endothermic dissolution of PPN at m = 0.6–1.0. In addition, the dissolution of PPN was found as entropy-driven at m = 0.8–1.0.

Supplementary Materials: The following are available online, Figure S1: Correlation of experimental solubility values of PPN with "Van't Hoff model" in different "THP + water" mixtures at "T = 298.2–318.2 K"; Van't Hoff model solubility values of PPN are represented by solid lines, and experimental solubility values of PPN are represented by the symbols, Table S1: Hansen solubility parameters (δ_{mix}/MPa$^{1/2}$) for various THP + water mixtures free of PPN at "T = 298.2 K", Table S2: The values of mixing enthalpy ($\Delta_{mix}H$/J mol^{-1}), mixing entropy ($\Delta_{mix}S$/J mol^{-1} K^{-1}), mixing Gibbs energy ($\Delta_{mix}G$/J mol^{-1}) and activity coefficient (γ_i) for PPN dissolution in different "THP + water" mixtures.

Author Contributions: Conceptualization and supervision, S.A.; Methodology, N.H., F.S. and S.A.; Validation, N.H. and F.S.; Writing—original draft, F.S. and S.A.; Writing—review and editing, N.H., F.S. and S.A.; Software, N.H. and F.S. All authors have read and agreed to the published version of the manuscript.

Funding: This research was funded by the Deanship of Scientific Research at King Saud University, Riyadh, Saudi Arabia via grant number RGP-1438-013, and the article processing charge (APC) was also supported by the Deanship of Scientific Research.

Acknowledgments: The authors would like to extend their sincere appreciation to the Deanship of Scientific Research at King Saud University, Riyadh, Saudi Arabia for funding this work through the research group project number RGP-1438-013.

Conflicts of Interest: The authors report no conflict of interest associated with this manuscript.

References

1. Vasavirama, K.; Upender, M. Piperine: A valuable alkaloid from piper species. *Int. J. Pharm. Pharm. Sci.* **2014**, *6*, 34–38.
2. Gorgani, G.; Mohammadi, M.; Najafpour, G.D.; Nikzad, M. Piperine-the bioactive compound of black pepper: From isolation to medicinal formulations. *Compr. Rev. Food Sci. Food Saf.* **2017**, *16*, 124–140. [CrossRef]
3. Pradeep, C.R.; Kuttan, G. Effect of piperine on the inhibition of lung metastatis induced B16F-10 melanoma cells in mice. *Clin. Exp. Metast.* **2002**, *19*, 703–708. [CrossRef] [PubMed]
4. Platel, K.; Srinivasan, K. Influence of dietary spices and their active principles on pancreatic digestive enzymes in albino rats. *Food/Nahrung.* **2000**, *44*, 42–46. [CrossRef]
5. Yang, Y.C.; Lee, S.G.; Lee, H.K.; Kim, M.K.; Lee, S.H.; Lee, H.S. A piperidine amide extracted from piper longum L. fruit shows activity against Aedes aegypti mosquito larvae. *J. Agric. Food Chem.* **2002**, *50*, 3765–3767. [CrossRef]
6. Piyachaturawat, P.; Glinsukon, T.; Peugvicha, P. Postcoital antifertility effect of piperine. *Contraception* **1982**, *26*, 625–633. [CrossRef]
7. Sethiya, N.K.; Shah, P.; Rajpara, A.; Nagar, P.A.; Mishra, S.H. Antioxidants and hepatoprotective effects of mixed micellar lipid formulation of phyllanthin and piperine in carbon tetrachloride-induced liver injury in rodents. *Food Funct.* **2015**, *6*, 3593–3603. [CrossRef]
8. Bai, Y.F.; Xu, H. Protective action of piperine against experimental gastric ulcer. *Acta Pharmacol. Sin.* **2000**, *21*, 357–359.
9. Meghwal, M.; Goswami, T.K. Piper nigrum and piperine: An update. *Compr. Phytother. Res.* **2013**, *27*, 1121–1130. [CrossRef]
10. Shamkuwar, P.B.; Shahi, S.R. Study of antidiarrhoeal activity of piperine. *Der Pharm. Lett.* **2012**, *4*, 217–221.

11. Ma, Z.G.; Yuan, Y.P.; Zhang, X.; Xu, S.C.; Wang, S.S.; Tang, Q.Z. Piperine attenuates pathological cardiac fibrosis via PPAR-γ/AKT pathways. *EBioMedicine* **2017**, *18*, 179–187. [CrossRef]
12. Moon, Y.S.; Choi, W.S.; Park, E.S.; Bae, I.K.; Choi, S.D.; Paek, O.; Kim, S.H.; Chun, H.S.; Lee, S.E. Antifungal and antiaflatoxigenic methylene-dioxy containing compounds and piperine-like synthetic compounds. *Toxins* **2016**, *8*, 240. [CrossRef]
13. Singh, N.K.; Saini, S.P.S.; Singh, H.; Jyoti; Sharma, S.K.; Rath, S.S. In vitro assessment of the acaricidal activity of piper longum, piper nigrum, and zingiber officinale extracts against hyalomma anatolicum ticks. *Exp. Appl. Acarol.* **2017**, *71*, 303–317. [CrossRef] [PubMed]
14. Sosa, S.; Balick, M.; Arvigo, R.; Esposito, R.; Pizza, C.; Altinier, G.; Tubaro, A. Screening of the topical anti-inflammatory activity of some Central American plants. *J. Ethnopharmacol.* **2002**, *81*, 211–215. [CrossRef]
15. Bang, J.S.; Choi, H.M.; Sur, B.J.; Lim, S.J.; Kim, J.Y.; Yang, H.I.; Yoo, M.C.; Hahm, D.H.; Kim, K.S. Anti-inflammatory and antiarthritic effects of piperine in human interleukin 1β-stimulated fibroblast-like synoviocytes and in rat arthritis models. *Arthritis Res. Ther.* **2009**, *11*, 1–9. [CrossRef]
16. Kaul, I.; Kapil, A. Evaluation of liver protective potential of piperine: An active principle of black pepper. *Planta Med.* **1993**, *59*, 413–417. [CrossRef] [PubMed]
17. Sabina, E.P.; Souriyan, A.D.H.; Jackline, D.; Rasool, M.K. Piperine, an active ingredient of black pepper attenuates acetaminophen-induced hepatotoxicity in mice. *Asian Pac. J. Trop. Dis.* **2010**, *3*, 971–976. [CrossRef]
18. Raman, G.; Gaikar, V.G. Microwave-assisted extraction of piperine from *Piper nigrum*. *Ind. Eng. Chem. Res.* **2002**, *41*, 2521–2528. [CrossRef]
19. Shoba, G.; Joy, D.; Joseph, T.; Majeed, M.; Rajendran, R.; Srinivas, P.S. Influence of piperine on the pharmacokinetics of curcumin in animals and human volunteers. *Planta Med.* **1998**, *64*, 353–356. [CrossRef]
20. Mujumdar, A.M.; Dhuley, J.N.; Deshmukh, V.K.; Naik, S.R. Effect of piperine on bioavailability oxyphenylbutazone in rats. *Indian Drugs* **1999**, *36*, 123–126.
21. Johnson, J.J.; Nihal, M.; Siddiqui, I.A.; Scarlett, C.O.; Bailey, H.H.; Mukhtar, H.; Ahmad, N. Enhancing the bioavailability of resveratrol by combining it with piperine. *Mol. Nutr. Food Res.* **2011**, *55*, 1169–1176. [CrossRef] [PubMed]
22. Shakeel, F.; Haq, N.; Salem-Bekhit, M.M.; Raish, M. Solubility and dissolution thermodynamics of sinapic acid in (DMSO + water) binary solvent mixtures at different temperatures. *J. Mol. Liq.* **2017**, *225*, 833–839. [CrossRef]
23. Shakeel, F.; Haq, N.; Siddiqui, N.A.; Alanazi, F.K.; Alsarra, I.A. Solubility and thermodynamic behavior of vanillin in propane-1,2-diol + water cosolvent at different temperatures. *Food Chem.* **2015**, *188*, 57–61. [CrossRef]
24. Shakeel, F.; Haq, N.; Siddiqui, N.A.; Alanazi, F.K.; Alsarra, I.A. Solubility and thermodynamics of vanillin in Carbitol-water mixtures at different temperatures. *LWT Food Sci. Technol.* **2015**, *64*, 1278–1282. [CrossRef]
25. Shakeel, F.; Haq, N.; Siddiqui, N.A.; Alanazi, F.K.; Alsarra, I.A. Thermodynamics of the solubility of reserpine in {{2-(2-ethoxyethoxy)ethanol + water}} mixed solvent systems at different temperatures. *J. Chem. Thermodyn.* **2015**, *82*, 57–60. [CrossRef]
26. Shakeel, F.; Haq, N.; Alanazi, F.K.; Alanazi, S.A.; Alsarra, I.A. Solubility of sinapic acid in various (Carbitol + water) systems: Computational modeling and solution thermodynamics. *J. Therm. Anal. Calorim.* **2020**, in press. [CrossRef]
27. Shakeel, F.; Alshehri, S.; Haq, N.; Elzayat, E.; Ibrahim, M.; Altamimi, M.A.; Mohsin, K.; Alanazi, F.K.; Alsarra, I.A. Solubility determination and thermodynamic data apigenin in binary {Transcutol® + water} mixtures. *Ind. Crops Prod.* **2018**, *116*, 56–63. [CrossRef]
28. Ezawa, T.; Inoue, Y.; Tunvichien, S.; Suzuki, R.; Kanamoto, I. Changes in the physicochemical properties of piperine/β-cyclodextrin due to the formation of inclusion complexes. *Int. J. Med. Chem.* **2016**, *2016*, E8723139. [CrossRef]
29. Khatri, S.; Awasthi, R. Piperine containing floating microspheres: An approach for drug targeting to the upper gastrointestinal tract. *Drug Deliv. Transl. Res.* **2016**, *6*, 299–303. [CrossRef]
30. Veerareddy, P.R.; Vobalaboina, V.; Nahid, A. Formulation and evaluation of oil-in-water emulsions of piperine in visceral leishmaniasis. *Pharmazie* **2004**, *59*, 194–197.
31. Shao, B.; Cui, C.; Ji, H.; Tang, J.; Wang, Z.; Liu, H.; Qin, M.; Li, X.; Wu, L. Enhanced oral delivery of piperine by self-emulsifying drug delivery systems: In vitro, in vivo and in situ intestinal permeability studies. *Drug Deliv.* **2015**, *22*, 740–747. [CrossRef] [PubMed]

32. Li, Q.; Zhai, W.; Jiang, Q.; Huang, R.; Liu, L.; Dai, J.; Gong, W.; Du, S.; Wu, Q. Curcumin-piperine mixtures in self-microemulsifying drug delivery system for ulcerative colitis therapy. *Int. J. Pharm.* **2015**, *490*, 22–31. [CrossRef] [PubMed]
33. Pentak, D. In vitro spectroscopic study of piperine-encapsulated nanosize liposomes. *Eur. Biophys. J.* **2016**, *45*, 175–186. [CrossRef]
34. Cherniakov, I.; Izgelov, D.; Barasch, D.; Davidson, E.; Domb, A.J.; Hoffman, A. Piperine-pro-nanolipospheres as a novel oral delivery system of cannabinoids: Pharmacokinetic evaluation in healthy volunteers in comparison to buccal spray administration. *J. Control. Release* **2017**, *266*, 1–7. [CrossRef]
35. Cherniakov, I.; Izgelov, D.; Domb, A.J.; Hoffman, A. The effect of pro nanolipospheres (PNL) formulation containing natural enhancers on the oral bioavailability of delta-9-tetrahydrocannabinol (THC) and cannabidiol (CBD) in a rat model. *Eur. J. Pharm. Sci.* **2017**, *109*, 21–30. [CrossRef] [PubMed]
36. Yusuf, M.; Khan, M.; Khan, R.A.; Ahmed, B. Preparation, characterization, in vivo and biochemical evaluation of brain targeted piperine solid lipid nanoparticles in an experimentally induced Alzheimer's disease model. *J. Drug Target.* **2013**, *21*, 300–311. [CrossRef]
37. Thenmozhi, K.; Yoo, Y.J. Enhanced solubility of piperine using hydrophilic carrier-based potent solid dispersion systems. *Drug Dev. Ind. Pharm.* **2017**, *43*, 1501–1509. [CrossRef] [PubMed]
38. Alshehri, S.; Haq, N.; Shakeel, F. Solubility, molecular interactions and mixing thermodynamic properties of piperine in various pure solvents at different temperatures. *J. Mol. Liq.* **2018**, *250*, 63–70. [CrossRef]
39. Raman, G.; Gaikar, V.G. Extraction of piperine from piper nigrum (black pepper) by hydrotropic solubilization. *Ind. Eng. Chem. Res.* **2002**, *41*, 2966–2976. [CrossRef]
40. Padalkar, K.V.; Gaikar, V.G. Extraction of piperine from piper nigrum (black pepper) by aqueous solutions of surfactant and surfactant + hydrotrope mixtures. *Sep. Sci. Technol.* **2008**, *43*, 3097–3118. [CrossRef]
41. Huang, X.; Lin, X.; Guo, M.; Zou, Y. Characteristics of piperine solubility in multiple solvent. *Adv. Mater. Res.* **2011**, *236–238*, 2495–2498. [CrossRef]
42. Kumoro, A.C.; Singh, H.; Hasan, M. Solubility of piperine in supercritical and near critical carbon dioxide. *Chin. J. Chem. Eng.* **2009**, *17*, 1014–1020. [CrossRef]
43. Apelblat, A.; Manzurola, E. Solubilities of o-acetylsalicylic, 4-aminosalicylic, 3,5-dinitrosalicylic and p-toluic acid and magnesium-DL-aspartate in water from T = (278–348) K. *J. Chem. Thermodyn.* **1999**, *31*, 85–91. [CrossRef]
44. Manzurola, E.; Apelblat, A. Solubilities of L-glutamic acid, 3-nitrobenzoic acid, acetylsalicylic, p-toluic acid, calcium-L-lactate, calcium gluconate, magnesium-DL-aspartate, and magnesium-L-lactate in water. *J. Chem. Thermodyn.* **2002**, *34*, 1127–1136. [CrossRef]
45. Yalkowsky, S.H.; Roseman, T.J. Solubilization of drugs by cosolvents. In *Techniques of Solubilization of Drugs*; Yalkowsky, S.H., Ed.; Marcel Dekker Inc.: New York, NY, USA, 1981; pp. 91–134.
46. Sotomayor, R.G.; Holguín, A.R.; Romdhani, A.; Martínez, F.; Jouyban, A. Solution thermodynamics of piroxicam in some ethanol + water mixtures and correlation with the Jouyban–Acree model. *J. Sol. Chem.* **2013**, *42*, 358–371. [CrossRef]
47. Jouyban, A. Review of the cosolvency models for predicting solubility of drugs in water-cosolvent mixtures. *J. Pharm. Pharm. Sci.* **2008**, *11*, 32–58. [CrossRef]
48. Babaei, M.; Shayanfar, A.; Rahimpour, E.; Barzegar-Jalali, M.; Martínez, F.; Jouyban, A. Solubility of bosentan in {propylene glycol + water} mixtures at various temperatures: Experimental data and mathematical modeling. *Phys. Chem. Liq.* **2019**, *57*, 338–348. [CrossRef]
49. Alshahrani, S.M.; Shakeel, F. Solubility data and computational modeling of baricitinib in various (DMSO + water) mixtures. *Molecules* **2020**, *25*, 2124. [CrossRef]
50. Higuchi, T.; Connors, K.A. Phase-solubility techniques. *Adv. Anal. Chem. Inst.* **1965**, *4*, 117–122.
51. Zhu, Q.N.; Wang, Q.; Hu, Y.B.; Abliz, X. Practical determination of the solubility parameters of 1-alkyl-3-methylimidazolium bromide ([CnC1im]Br, n = 5, 6, 7, 8) ionic liquids by inverse gas chromatography and the Hansen solubility parameter. *Molecules* **2019**, *24*, 1346. [CrossRef]
52. Shakeel, F.; Haq, N.; Alsarra, I.A.; Alshehri, S. Solubility, Hansen solubility parameters and thermodynamic behavior of emtricitabine in various (polyethylene glycol-400 + water) mixtures: Computational modeling and thermodynamics. *Molecules* **2020**, *25*, 1559. [CrossRef] [PubMed]

53. Wan, Y.; He, H.; Huang, Z.; Zhang, P.; Sha, J.; Li, T.; Ren, B. Solubility, thermodynamic modeling and Hansen solubility parameter of 5-norbornene-2,3-dicarboximide in three binary solvents (methanol, ethanol, ethyl acetate + DMF) from 278.15 K to 323.15 K. *J. Mol. Liq.* **2020**, *300*, E112097. [CrossRef]
54. Smith, J.M.; Ness, H.C.V.; Abbott, M.M. *Introduction to Chemical Engineering Thermodynamics*; McGraw-Hill: New York, NY, USA, 2001.
55. Li, X.; Cong, Y.; Du, C.; Zhao, H. Solubility and solution thermodynamics of 2-methyl-4-nitroaniline in eleven organic solvents at elevated temperatures. *J. Chem. Thermodyn.* **2017**, *105*, 276–288. [CrossRef]
56. Zhao, K.; Yang, P.; Du, S.; Li, K.; Li, X.; Li, Z.; Liu, Y.; Lin, L.; Hou, B.; Gong, J. Determination and correlation of solubility and thermodynamics of mixing of 4-aminobutyric acid in mono-solvents and binary solvent mixtures. *J. Chem. Thermodyn.* **2016**, *102*, 276–286. [CrossRef]
57. Vanderbilt, B.M.; Clayton, R.E. Bonding of fibrous glass to elastomers. *Ind. Eng. Chem. Prod. Res. Dev.* **1965**, *4*, 18–22. [CrossRef]
58. Ruidiaz, M.A.; Delgado, D.R.; Martínez, F.; Marcus, Y. Solubility and preferential solvation of indomethacin in 1,4-dioxane + water solvent mixtures. *Fluid Phase Equilib.* **2010**, *299*, 259–265. [CrossRef]
59. Manrique, Y.J.; Pacheco, D.P.; Martínez, F. Thermodynamics of mixing and solvation of ibuprofen and naproxen in propylene glycol + water cosolvent mixtures. *J. Sol. Chem.* **2008**, *37*, 165–181. [CrossRef]
60. Shakeel, F.; Alshehri, S.; Imran, M.; Haq, N.; Alanazi, A.; Anwer, M.K. Experimental and computational approaches for solubility measurement of pyridazinone derivative in binary (DMSO + water) systems. *Molecules* **2020**, *25*, 171. [CrossRef]
61. Hildebrand, J.H.; Prausnitz, J.M.; Scott, R.L. *Regular and Related Solutions*; Van Nostrand Reinhold: New York, NY, USA, 1970.
62. Jouyban, A.; Chan, H.K.; Chew, N.Y.; Khoubnasabiafari, N.; Acree, W.E., Jr. Solubility prediction of paracetamol in binary and ternary solvent mixtures using Jouyban-Acree model. *Chem. Pharm. Bull.* **2006**, *54*, 428–431. [CrossRef]
63. Jouyban, A.; Acree, W.E., Jr. In silico prediction of drug solubility in water-ethanol mixtures using Jouyban-Acree model. *J. Pharm. Pharm. Sci.* **2006**, *9*, 262–269.
64. Khoubnasabjafari, M.; Shayanfar, A.; Martínez, F.; Acree, W.E., Jr.; Jouyban, A. Generally trained models to predict solubility of drugs in carbitol + water mixtures at various temperatures. *J. Mol. Liq.* **2016**, *219*, 435–438. [CrossRef]
65. Jouyban, A.; Fakhree, M.A.A.; Acree, W.E., Jr. Comment on "Measurement and correlation of solubilities of (*Z*)-2-(2-aminothiazol-4-yl)-2-methoxyiminoacetic acid in different pure solvents and binary mixtures of water + (ethanol, methanol, or glycol)". *J. Chem. Eng. Data* **2012**, *57*, 1344–1346. [CrossRef]
66. Jouyban-Gharamaleki, A.; Hanaee, J. A novel method for improvement of predictability of the CNIBS/R-K equation. *Int. J. Pharm.* **1997**, *154*, 245–247. [CrossRef]

Sample Availability: Samples of the compound PPN are available from the authors.

© 2020 by the authors. Licensee MDPI, Basel, Switzerland. This article is an open access article distributed under the terms and conditions of the Creative Commons Attribution (CC BY) license (http://creativecommons.org/licenses/by/4.0/).